Pernas-Sánchez, J.; Artero-Guerrero, J. A.; Varas, D.; López-Puente, J. (2014). "Experimental analysis of normal and oblique high velocity impacts on carbon/ epoxy tape laminates". *Composites Part A: Applied Science and Manufacturing*, v. 60, May, pp. 24-31.
DOI: 10.1016/j.compositesa.2014.01.006

Proyectos:

DPI2010-15123

CCG10-UC3M/DPI-4694

Experimental analysis of normal and oblique high velocity impacts on carbon/epoxy tape laminates

J. Pernas-Sánchez, J.A. Artero-Guerrero, D. Varas,

Department of Continuum Mechanics and Structural Analysis. University Carlos III of Madrid. Avda. de la Universidad, 30. 28911 Leganés, Madrid, Spain

Key words: Obliquity; high velocity impact; tape laminate; carbon/epoxy.

Abstract

In this work, the effect of high velocity impacts on carbon/epoxy tape quasi-isotropic laminates is studied. Experimental test were carried out at two different impact angles and in a wide range of velocities (from 80 to 490 m/s). Both parameters, the residual velocity and the damaged area, are used to evaluate the effect of the kinetic energy of the projectile on the laminate response. In addition it has been proposed a simplified analytical model which allows to identify the different energy absorbtion mechanisms and predict the residual

* Corresponding author. Fax number: 34 916248881. E-mail address: jlpuente@ing.uc3m.es

velocity of the projectile. Finally the energy absorbed by the laminate during the impact is studied.

1 Introduction

Carbon/epoxy composite laminates are widely used in transport industries due to their excellent mechanical properties and low density compared with metallic materials. The automotive industry has focused its attention on those materials in order to diminish the weight of the structure and hence the fuel consumption. The high speed train industry, is also focusing its attention on those materials in order to develop lighter structures, allowing speed increase and lower energy consumption. Finally the aerospace and the aeronautic industries are the ones that are using carbon/epoxy composite laminates in many structural parts (up to 50 % in weight in the latest aircraft developments); nevertheless it is possible to increase the percentage of those materials in the aircraft structures. Aeronautic and aerospace industries are very interested in the analysis of how their structures behave [1] under different kinds of impacts phenomenon such as hail [2], rubber [3] or even turbine blades [4] impacts, HRAM [5–9] since their reliability requirements are very high.

The analysis of the high velocity impact on carbon/epoxy laminates has been studied since the 80's with a few works. Cantwell and Morton [10] published in 1985 a seminal work regarding the high velocity impacts on composite laminates; they analyzed different non-destructive techniques in order to explore the merits and weaknesses of each method. Later in 1989 [11,12] they studied the main differences between low and high velocity impacts; in those works they show that high velocity impacts are not governed by the specimen size, and in addition suggest that those impacts are more detrimental to the integrity of a composite structure than low velocity. In the following decade Lee and Sun [13] analyzed the high velocity impact of blunt projectiles and obtained its ballistic limit for different thickness. In 1996 Sun and Potti [14] analyzed the high velocity impact of blunt projectiles on thick laminates, and in addition they developed a model to predict the residual velocity in case of perforation with high accuracy. The following year, Larsson [15] studied the effect of stitching in the behavior of carbon/epoxy laminates under high velocity impacts, concluding that its resistance to delamination was larger.

In the next decade the number of articles regarding high velocity impacts on carbon/epoxy laminates grew substantially, and not always the main focus was experimental, many of them had a numerical [16–21] or an analytical point of view [22–26], which is not the main porpoise of the current work.

In 2001 Bland and Dear [27] published a very interesting article comparing the damage induced by high and low velocity impacts, as well as the deflection of the laminate. Lopez et al. [28] in 2002 studied the influence of the low temperature in the behavior of both tape and woven carbon/epoxy laminates under high velocity impacts, concluding that the lower temperature promotes larger damage. Will et al. [29] analyzed the influence of stacking sequence on tubes subjected to high velocity impacts, stating that the influence of the ply orientation was small. Tanabe et al. [30] analyzed the influence on different carbon fibres in the behaviour under impact of carbon/epoxy laminates. Recently Zhao et al. [31] studied the behavior of carbon/epoxy woven laminates under high velocity impacts; during the test they placed strain gauges and observed that its magnitude was proportional to the impact velocity.

Regarding the analysis of the influence of obliquity in high velocity impacts on carbon/epoxy laminates the available information is much more scarce. In the literature it was possible only to find very few articles [32–34] that analyze the effect of the impact trajectory, being all of them for woven laminates. Therefore it is necessary to study the effect of oblique impacts on quasi-isotropic unidirectional composites to improve the structural design that uses those kind of laminates.

The objective of this work is to analyze the high velocity impact phenomenon on carbon/epoxy unidirectional composites, and how the obliquity affects the laminate response. To this end, it is important to know which failure mechanisms participate in the process and in addition which is their relative importance. The first step will be to use experimental tests to visualize an explore the mechanisms that appear in the laminate; then a energy balance will be used to quantify the different failure mechanisms.

2 Experimental methodology

In order to study the effect of high velocity impact on carbon/epoxy tape laminates, the first step is to perform experimental tests in a wide range of impact velocity and with two different impact angles 0^o and 45^o. Composite laminates used in this study were manufactured by Sacesa, from prepregs made by Hexcel composites; the carbon fibre was AS4 and the epoxy matrix corresponds to the 8552 series. A quasi-isotropic configuration with 12 plies (+45/-45/0/90/90/0)s and a total thickness of 2.4 mm was chosen; this configuration is commonly used when there is not a preferential load direction, which makes the laminate useful for many applications. The test coupons size were $110 \times 110 mm^2$; this size is the smallest one which assures that the damage of the composite does not reach its contour. The laminates were simply supported. In addition the ratio laminate size over projectile diameter is greater or equal than the ratios used in other works [35–37]. The projectile used was a steel sphere of 7.5 mm diameter and 1.73 g of mass; it is tempered, and its strength is high enough to avoid plastic deformation during the impact process. Spherical shape was adopted in order to avoid scattered result due to yaw angle during the projectile flight.

In order to accomplish the experimental tests a pneumatic launcher was employed; this experimental device uses helium up to pressures of 200 bar to impel the projectile. Since the diameter of the barrel was 7.62 mm, the use of a sabot was not necessary. In order to measure the impact and the residual velocity, a high speed video camera (Photron Ultima APX-RS) was used; since the exposure time was very small (10 μs), a 1200 W HMI lamp was used to assure enough lighting. The camera was configured to obtain 36000 fps. Using this set-up the obtention of the impact and the residual velocity was easy and reliable. Fig. 1 shows an example of a video sequence of normal impact at 223 m/s of velocity.

Fig. 1. Impact sequence from a normal impact at 223 m/s.

One of the most important variables when a projectile impacts to a composite laminate is the induced damage. The C-Scan technique was used to measure the damaged area; this nondestructive inspection method allows to perform an accurate quantification of the damage extent. Usually the area of this damage could be lately related to the laminate strength reduction by using damage tolerance theories, which are not the main purpose of this work. The only drawback of this method is the impossibility of distinguish the type of damage (matrix cracking, matrix crushing, delamination or fiber failure) and where it is situated along the thickness since it provides a projection of the damage presented in all the plies. To avoid this limitations, after the C-Scan inspection, laminates were carefully cut along a transverse plane, at the impact point. A simple photograph of the laminate cross-section, allows the possibility to determine the type of damage and its localization along the thickness.

3 Experimental inspection of laminates

In this section an analysis of the different breakage mechanisms that appear on those previously impacted composite laminates is accomplished. For a better understanding of the processes that occur when a high velocity projectile impacts the carbon/epoxy tape panel, two different regimes are studied: impact velocities below and above ballistic limit. The ballistic limit (v_{bl}) is defined as the minimum impact velocity, for a given projectile/composite pair and impact angle, that produces complete penetration. In this work, two different impact angles are studied, and hence two different ballistic limits values are defined, being lower the one related with normal impact.

3.1 Impacts below ballistic limit

When the impact velocity is not high enough to perforate the laminate, it is assumed that the composite absorbs all the kinetic energy of the projectile mainly in form of damage. The ballistic limit is around 120 m/s for normal impacts and around 140 m/s for oblique impacts. Tape laminates in quasi-isotropic ply lay-out exhibit large delamination area when subjected to transverse impact at this range of velocities. When local bending is induced in the composite panel by the impact, some plies try to bend more than others. This behavior is due to the different apparent bending stiffness between the plies that have different orientation [38]; this promotes a separation of the plies and hence the apparition of the delamination. As the laminate bends, the inter-ply shear stresses promote the growth of the delamination.

Figs. 2(a) and 2(b) show respectively the cross-section of normal and oblique impacted laminates at velocities around 85 m/s; the impact occurs in the upper face, and the trajectory of the oblique one comes from right. Both of them exhibit matrix crushing along the projectile direction; the zone affected by this kind of damage is larger in the normal impact case. Delamination is also observed in both impacts, mainly between the last two plies.

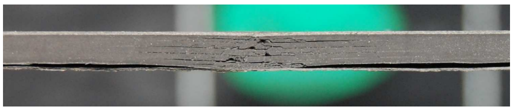

(a) 0^o impact, $85m/s < v_{bl}$.

(b) 45^o impact, $83m/s < v_{bl}$.

(c) 0^o impact, $153m/s > v_{bl}$.

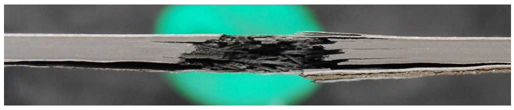

(d) 45^o impact, $157m/s > v_{bl}$.

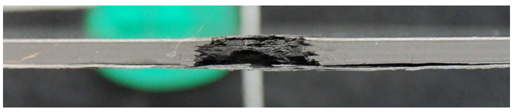

(e) 0^o impact, $492m/s > v_{bl}$.

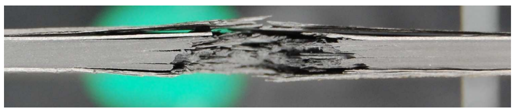

(f) 45^o impact, $493m/s > v_{bl}$.

Fig. 2. Images of cross-section of impacted laminates.

Cross-section images are useful in order to visualize the type of damage that appears in the laminate; nevertheless in order to quantify the damage extension, C-Scan images are much useful. Figs. 3(a) and 3(b) show respectively the C-Scan image of normal and oblique impacts; the dark area indicates the damaged zone, which is larger in the normal impact. The values of the damaged areas are shown in Fig.

In this kind of images is not possible to differentiate which kind of damage is presented, but using the cross-section images it is possible to say that is mainly delamination.

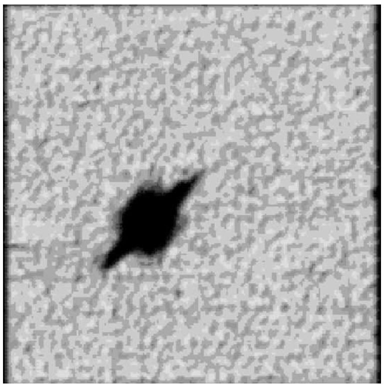

(a) 0^o impact, $85m/s < v_{bl}$.

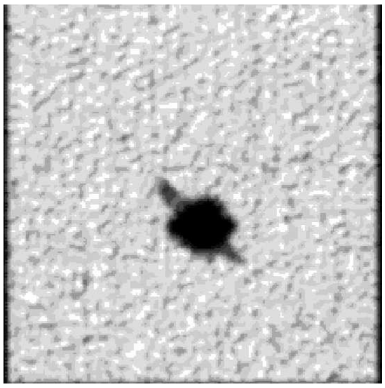

(b) 45^o impact, $83m/s < v_{bl}$.

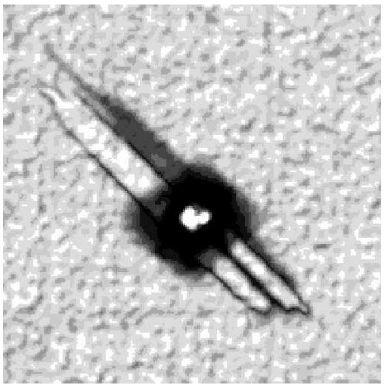

(c) 0^o impact, $153m/s > v_{bl}$.

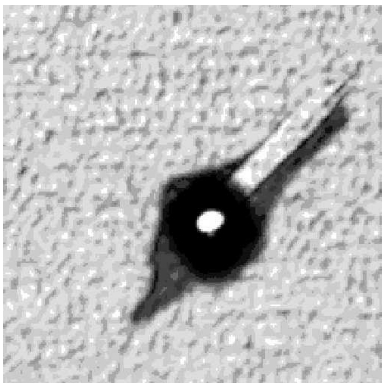

(d) 45^o impact, $157m/s > v_{bl}$.

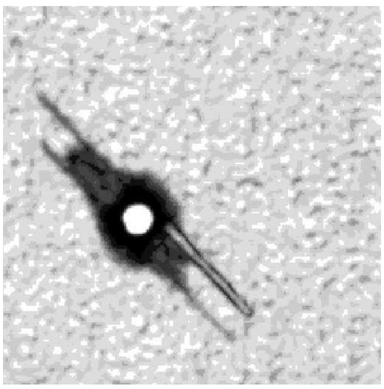

(e) 0^o impact, $492m/s > v_{bl}$.

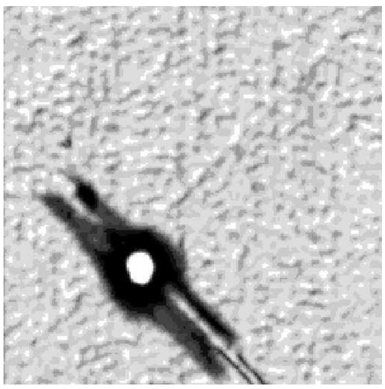

(f) 45^o impact, $493m/s > v_{bl}$.

Fig. 3. C-Scan images of impacted laminates.

3.2 Impacts above ballistic limit

When the impact velocity of the projectile is high enough to perforate the unidirectional quasi-isotropic laminate, the difference between the initial and the residual kinetic energy of the projectile is the energy absorbed by the laminate. In this case the energy absorbed by the laminate is not only delamination and matrix crushing. Some part of the energy is absorbed by matrix and fiber failure (to create the plug) and some other is used to accelerate the plug (linear momentum transfer) from rest to the projectile residual velocity. Figs. 2(c) and 2(d) show respectively the cross-section of normal and oblique impacted laminates at velocities around 155 m/s; in this case full perforation is achieved in both cases. The perforation cone is straight in the normal impact and crooked in the direction of the impact for the oblique one (the trajectory comes from the right side); hence the plugs ejected during the impact process are supposed to be like a truncated cone. Delamination is presented in both cases in many inter-plies zones. The corresponding C-Scan images of those two impacts are presented in Figs. 3(c) (normal) and 3(d) (oblique); the white area represents the hole made by the impact. Here the damage extension is much greater compared to the previous velocity analyzed, and the oblique case presents larger damaged area than the normal case.

Finally, at very high velocities the damage induced by the projectile is much more localized around the impact point; this means that the damaged area is smaller than at lower velocities (above ballistic limit). Figs. 2(e) and 2(f) show the cross section of impacts occurred around 490 m/s; here the delamination is very small compared to the 155 m/s case, being larger in the oblique case. Figs. 3(e) and 3(f) shows the corresponding C-Scan images; as aforementioned the damage for the oblique case is larger than for the normal case, and both are smaller than the impact at 155 m/s.

4 Analysis of experimental tests

The images of impacted laminates obtained by the C-Scan allow measuring the damaged area using an image processor software and hence represent the damaged area vs. the impact velocity for both normal and oblique impacts cases, Fig. 4.

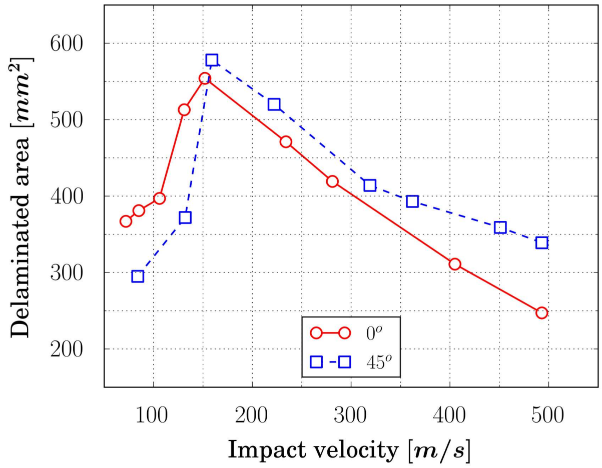

Fig. 4. Damaged area vs. impact velocity for normal and oblique impacts.

It is observed that the damaged area for both impact angle cases increases with the impact velocity up to approximately the moment in which the projectile perforates the laminate, from that moment the projectile passes through the plate and the damaged area diminishes as the impact velocity increases obtaining a damaged area equivalent to the perfect hole of the projectile. However, different trends are observed for the different impact angles regarding the impact velocity. Below the ballistic limit, the normal impacts perform higher damage than the oblique impacts. The reason of this behavior is that the normal force applied by the projectile is the principal component that induces damage due to the smaller strength of the laminate in the through-thickness direction; for the same impact velocity this normal component is larger in the case of normal impacts, Fig. 5. At impact velocities above the ballistic limit, the trend changes so that the oblique impacts perform higher damaged area that the normal impacts. This can be explained taking into account that when the impact occurs at very high velocity the projectile makes a perfect hole in the laminate. In the oblique cases the trajectory through the laminate promotes an elliptical shaped damaged area, whereas the normal impact promotes a circled one. It is possible to say that the ratio between the two areas in case of very high impact velocity will be $\left(r\sqrt{2}+h/2\right)/r$.

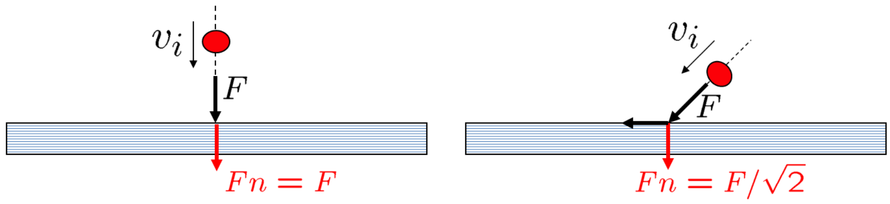

(a) Impacts below ballistic limit.

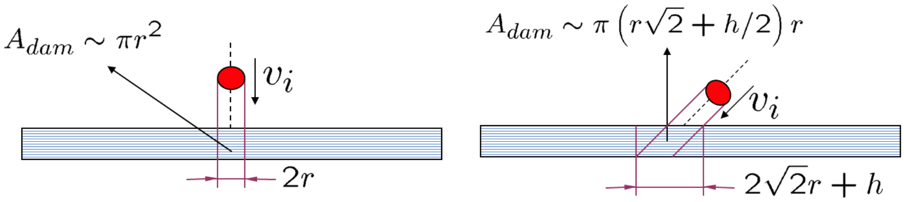

(b) Impacts above ballistic limit, at very high velocities.

Fig. 5. Sketch of the impact on composite laminates.

5 Energy absorbed by the composites

Once the damage mechanisms that appear during the impact process have been identified, it is possible to perform an analysis of how the kinetic energy of the projectile is absorbed by the composite laminate.

5.1 Introduction

In order to evaluate the energy absorbed by the laminate during the impact it is necessary to use the impact and the residual velocity of the projectile, which was measured (as aforementioned) by means of a high speed video camera. Fig. 6 shows the residual velocity vs. impact velocity for both normal and oblique impacts, and the fitting curves (with $R^2 > 0.99$) used for this type of data using the Lambert-Jonas equation: $v_r = A \;\; v_i^p - v_{bl}$ where v_r is the residual velocity, v_i the impact velocity and v_{bl}, A and p are the fitting parameters. Using this regression curves an accurate value for the ballistic limit is obtained: 118 m/s for normal impacts and 139 m/s for oblique impacts. This expression has significance only for $v_i > v_{bl}$.

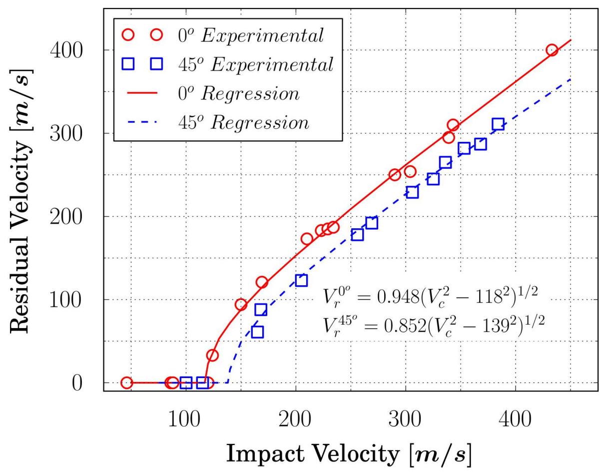

Fig. 6. Residual velocity vs. impact velocity for normal and oblique impacts, including regression curves.

5.2 Energy balance

The analysis of the experimental results allows to consider that the kinetic energy of the projectile E_k is absorbed by the laminate through three different mechanisms: linear momentum transfer E_{lm}, delamination E_d and laminate crushing E_c. Let's analyze those three contributions:

- *linear momentum transfer:* when the projectile penetrates the laminate (the impact velocity is above the ballistic limit) it is considered that it accelerates the detached laminated from the rest to the same residual velocity of the projectile. This phenomenon has been observed by Hazell et al. [33]. The laminate mass accelerated is the plug generated during the impact and could be estimated as $\pi\, r^2\, h\, \rho_l$ where r is the projectile radius, h is the laminate thickness and ρ_l the laminate density. The energy absorbed through this mechanism is equal to the final kinetic energy of the plug which is $E_{lm} = 1/2\pi\, r^2\, h\, \rho_l\, v_r^2$. This magnitude does not change if the impact is oblique since the volume of the plug created is the same.

- *delamination:* the analysis of the impacted laminates showed a delamination area which is maximum at impact velocities close to the ballistic limit. The energy absorbed through this mechanism could be estimated as $E_d = K\, A_d\, G_{II}$ where A_d is the delaminated area, K is the number of delaminated interfaces and G_{II} is the energy absorbed due to delamination, which is a material property. It is assumed that delamination mainly occur in mode II since there is no tension force applied in the direction perpendicular to the laminate plane (in addition its value is much larger than mode I). This expression is valid for both normal and oblique impacts.

- *laminate crushing:* this mechanism represents the energy consumed in the breakage of the laminate, and hence the formation of the plug. This term could be estimated as the force applied by the projectile multiplied by the distance: $E_c = \sigma_c(\alpha)\;\pi\, r^2\, \bar{h}(\alpha)$. In this expression $\sigma_c(\alpha)$ is the crushing strength which is function of the impact angle, and $\bar{h}(\alpha)$ is the distance traveled by the projectile inside the laminate which is also function of the obliquity.

The balance equation then could be written as:

$$\frac{1}{2}\, m_p\, v_i^2 - \frac{1}{2}\, m_p\, v_r^2 = \frac{1}{2}\, \pi\, r^2\, h\, \rho_l\, v_r^2 + K\, A_d\, G_{II} + \sigma_c(\alpha)\;\pi\, r^2\, \bar{h}(\alpha) \tag{1}$$

There are two terms that depend on the impact angle

$\bar{h}(\alpha)$ and $\sigma_c(\alpha)$. The first one is easily related with the obliquity, by the fact that is the trajectory followed by the projectile: $\bar{h}(\alpha) = h/cos\alpha$ (being $\alpha = 0$ the normal impact). In order to relate the crushing stress with the impact angle the expression to be used is:

$$\sigma_c(\alpha) = \sqrt{\frac{4}{\frac{(1+cos2\alpha)^2}{(\sigma_c^0)^2} + \frac{(1-cos2\alpha)^2}{(\sigma_c^{90})^2} + \frac{(sin2\alpha)^2}{(\tau_c^{0,90})^2}}} \tag{2}$$

In a previous work [32] there is a complete description of how this expression is obtained. The parameters σ_c^0, σ_c^{90} and $\tau_c^{0,90}$ are respectively the crushing strength in the through-thickness direction, in the direction of the fibers and under shear. Dividing Eq. (1) by the kinetic energy of the projectile and rearranging:

$$\left(\frac{v_r}{v_i}\right)^2 = \frac{m_p}{\pi\, r^2\, \rho_l\, h + m_p} - \frac{2\, K\, A_d\, G_{I-II}}{v_i^2\,(\pi\, r^2\, h\, \rho_l + m_p)} - \frac{2\,\sigma_c(\alpha)\,\bar{h}(\alpha)\;\pi\, r^2}{v_i^2\,(\pi\, r^2\, h\, \rho_l + m_p)} \tag{3}$$

Eq. (3) is dimensionless, so it is possible to analyze the relative importance of the three terms that appear at the right side of the equation substituting the values of the parameters, Eq. 4. The table 1 shows the values of the problem that has been used; the material constants were obtained from the literature [20,39].

$$\begin{cases} \dfrac{m_p}{\pi\, r^2\, \rho_l\, h + m_p} \sim 1 \\[2em] \dfrac{2\, K\, A_d\, G_{II}}{v_i^2\,(\pi\, r^2\, h\, \rho_l + m_p)} \sim \dfrac{200}{v_i^2} \\[2em] \dfrac{2\,\sigma_c(\alpha)\,\bar{h}(\alpha)\;\pi\, r^2}{v_i^2\,(\pi\, r^2\, h\, \rho_l + m_p)} \sim \dfrac{2000}{v_i^2} \end{cases} \tag{4}$$

It is clear that the second term is 10 times smaller than the third one and hence could be neglected. The residual velocity could be calculated then by:

$$v_r = \sqrt{\frac{m_p\, v_i^2}{\pi\, r^2 \rho_l\, h + m_p} - \frac{2\,\sigma_c(\alpha)\,\bar{h}(\alpha)\;\pi\, r^2}{\pi\, r^2 \rho_l\, h + m_p}} \tag{5}$$

variable	value
$h \quad [m]$	2.4×10^{-3}
$\sigma_c^0 \quad [N/m^2]$	1.2×10^8
$\sigma_c^{90} \quad [N/m^2]$	1.4×10^8
$\tau_c^{0,90} \quad [N/m^2]$	1.0×10^8
$\sigma_c \quad [N/m^2]$	$\sim 1.3 \times 10^8$
$A_d \quad [m^2]$	4×10^{-4}
$m_p \quad [kg]$	1.7×10^{-3}
$\rho_l \quad [kg/m^3]$	1500
$r \quad [m]$	3.75×10^{-3}
$G_{II} \quad [N/m]$	750
K	2

Table 1

Values of the constants that appear in the problem.

Finally it is possible to obtain the value of the ballistic limit, using Eq. 5 and setting the residual velocity equal to zero. The expression obtained for the ballistic limit is:

$$v_{bl} = \sqrt{\frac{2\,\sigma_c\,(\alpha)\,\bar{h}\,(\alpha)\;\pi r^2}{m_p}} \tag{6}$$

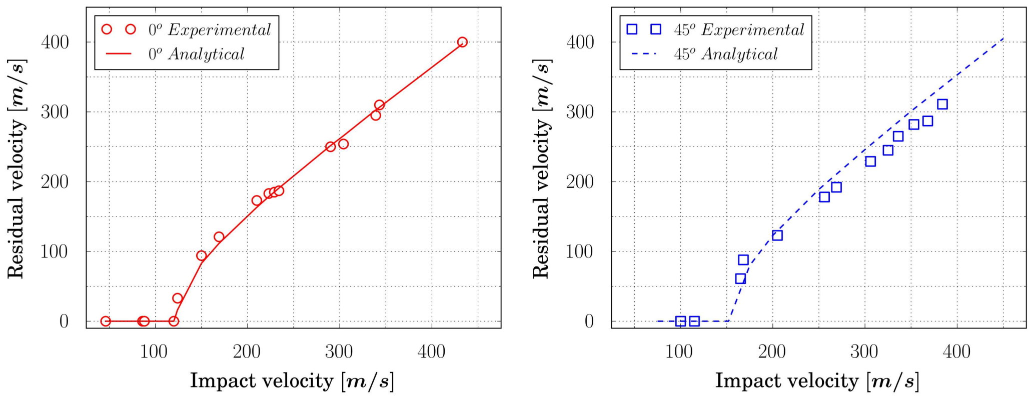

(a) (b)

Fig. 7. Residual velocity vs. impact velocity for experimental data and model data; a): normal impact, b): oblique impact.

5.3 Model validation

In order to evaluate if the model gives accurate values of residual velocity, Fig. 7 shows a comparison between the experimental results and the results given by Eq. (5). For both cases normal and oblique impacts the results are accurate.

Now that the model is validated it is possible to analyze how the curves of residual velocity vs. impact velocity vary with the impact angle. Fig. 8 (a) shows different curves for every 15^o of impact angle up to 60^o. It is important to note that the results at impact angles of 60^o should be taken carefully, since no experimental test above 45^o are available. Nevertheless the results for that impact angle are shown in order to have a wider view of the impact angle influence. For low impact angles the differences of the residual velocity are very small, but as soon as the angle increases the differences tend to be larger, mainly in the range of velocities in which the laminate is not perforated, near the ballistic limit. This behavior is due to the increase of the projectile trajectory that strongly increases for larger angles and makes more difficult the projectile to perforate the laminate. Once the projectile perforates the laminate, the residual velocity tends to an asymptotic value independently of the impact angle; the reason for this behavior will be explained later. Fig. 8 (b) shows how the ballistic limit varies with the impact angle; for low obliquity the variation is small, but as soon as the angle reaches values of 30^o the ballistic limit increases up to 1.5 times the value for normal impact.

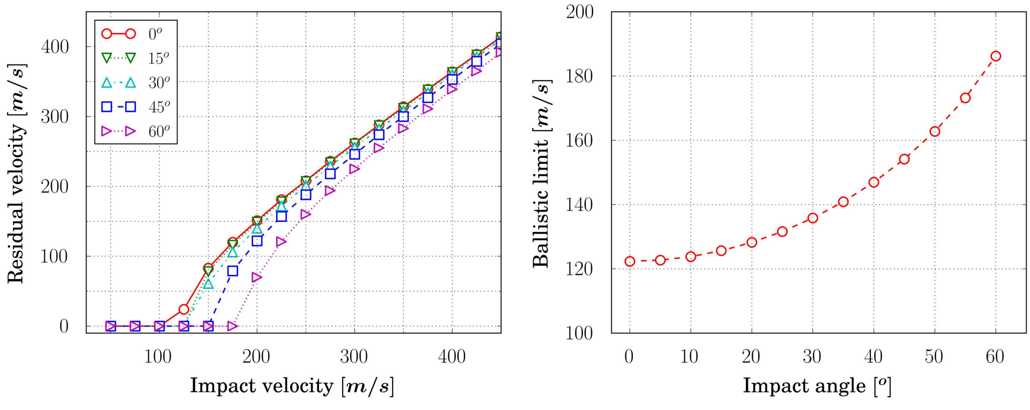

(a) (b)

Fig. 8. Residual velocity vs. impact velocity for different impact angles and variation of the ballistic limit with the impact angle.

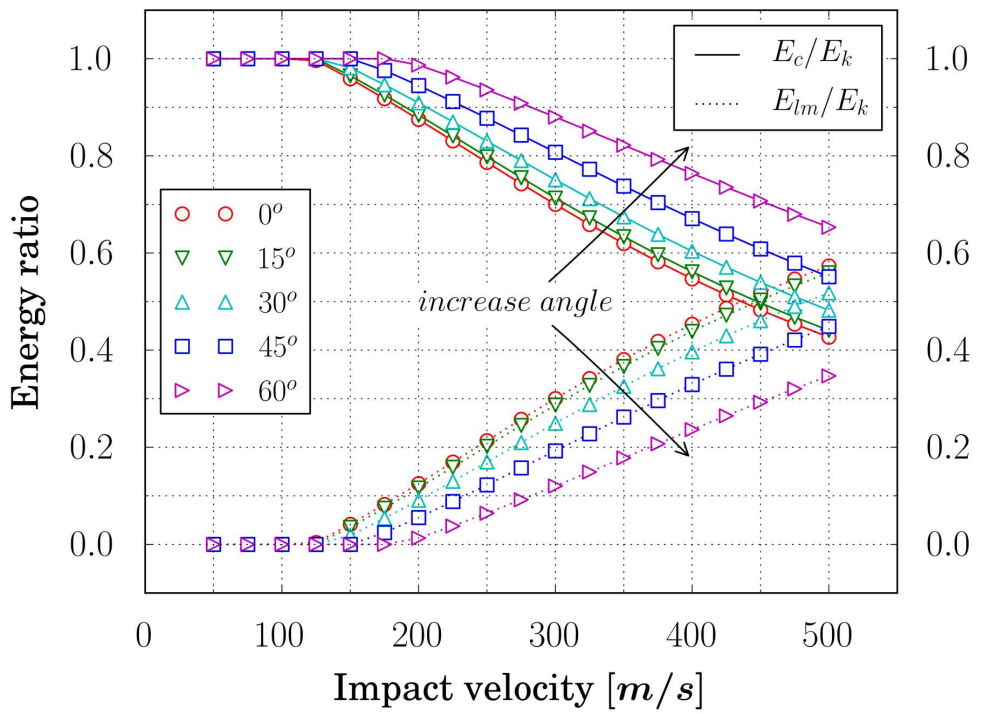

Fig. 9. Energy absorbed mechanism as function of the impact velocity for different impact angles.

Another interesting analysis is the evaluation of how the laminate absorbs the kinetic energy of the projectile (E_k), Fig. 9. At low velocities, below ballistic limit all the energy is absorbed through laminate crushing (E_c), since there is no plug formation. As the impact velocity increases above the ballistic limit the energy absorbed by linear momentum transfer (E_{lm}) increases, whereas the energy absorbed by laminate crushing stays constant (for a given impact angle) since it does not vary with the impact velocity . Since the linear momentum transfer does not change with the impact angle, it is expected that the laminate crushing increases in importance with the impact angle; this is clear in the Fig. 9.

Finally the Fig. 10 shows the energy absorbed by the laminate (E_{abs}) over the projectile kinetic energy as function of the impact velocity; at velocities below ballistic limit the ratio is one since all the kinetic energy of the projectile is absorbed by the laminate. The curves for the different impact angles seems to have the same shape but moved in the x axis. As the velocity goes beyond ballistic limit, the ratio diminishes tending to an asymptotic value. This behavior could be explained taking into account that at very high velocities the main absorbtion mechanism is due to the linear momentum transfer (see Eq. 4) and hence the residual velocity could be estimated (from Eq. 5) as: $v_r = v_i \quad m_p/\left(\pi\, r^2 \rho_l\, h + m_p\right)$; this is the asymptotic line to which all residual velocity curves tend at high impact velocities (Fig. 8(a)). Then at very high velocities:

$$\frac{E_{abs}}{E_k} = \frac{0.5\, m_p v_i^2 - 0.5\, m_p v_r^2}{0.5\, m_p v_i^2} = \frac{\pi\, r^2 \rho_l\, h}{\pi\, r^2 \rho_l\, h + m_p} \tag{7}$$

Which for the values used in this work means that the asymptotic value is $E_{abs}/E_k \sim 0.0855$.

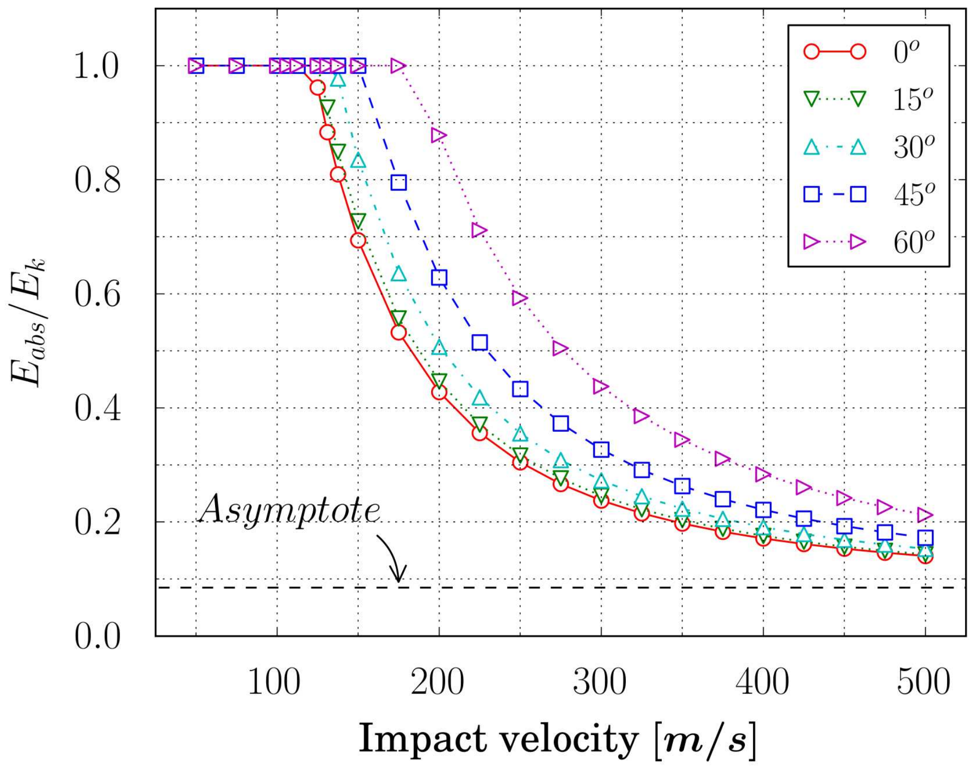

Fig. 10. absorbed energy over the kinetic projectile energy as function of the impact velocity.

6 Conclusions

In this work, the analysis of high velocity impacts on unidirectional composites has been accomplished. High-velocity impact tests have been performed in a wide range of velocities and with two impact angles; then the damage mechanisms have been analyzed using both destructive and non-destructive techniques. In order to understand the contribution of the damage mechanisms in terms of absorbed energy, an analytical model has been proposed. From these results presented and discussed, the main conclusions are as follows:

- At velocities below the ballistic limit the damage induced by the oblique impacts is smaller than the one promoted by normal impacts; in this range is the normal component of the impact force the one that causes damage. At velocities above ballistic limit the behavior is the opposite; in this case the oblique trajectory during penetration of the projectile promotes a larger damaged area.

- An analytical model has been developed and then validated. It is capable to predict the residual velocity of the projectile in case of penetration, and in addition the energy absorbed during the impact. The model allows to obtain results for different impact angles with a very low computational cost.

- The main energy absorbtion mechanisms that appear during the impact are: linear momentum transfer, delamination and laminate crushing. Even if the delamination is the most dangerous because affects a large area of the laminate, it has been seen that in the cases studied is the one that absorbs less energy and its contribution is negligible compared to the linear momentum transfer or the laminate crushing.

  The relative importance of the energy absorbtion mechanism varies significantly with the impact angle. It has been shown that for a given impact velocity, as soon as the impact angle grows, the energy absorbed by laminate crushing increases in importance whereas the one absorbed by linear momentum transfer diminishes.

Acknowledgements

This research was done with the financial support of the Spanish Ministry of Education under Project reference DPI2010-15123 and of the Region of Madrid and University Carlos III of Madrid under Project reference CCG10-UC3M/DPI-4694.

References

[1] Avery JG. AGARD, Design Manual for Impact Damage Tolerant Aircraft Structure, Technical Editing and Reproduction Ltd, London, UK, 1981.

[2] Anghileri M, Castelleti LML, Invernizzi F, Mascheroni M. A survey of numerical models for hail impact analysis. International Journal of Impact Engineering 31 (2005) 929–944.

[3] Mines RAW, McKown S, Birch RS. Impact of aircraft rubber tyre fragments on aluminium alloy plates: I-experimental. International Journal of Impact Engineering 34 (2007) 627–646.

[4] Hai-jun X, Rong-ren W. Aeroengine turbine blade containment tests using hig-speed rotor spin test facility. Aerospace Science and Technology 10 (2006) 501–508.

[5] Varas D, López-Puente J, Zaera R. Experimental analysis of fluid-filled aluminium tubes subjected to high-velocity impact. International Journal of Impact Engineering 36 (2009) 81–91.

[6] Varas D, López-Puente J, Zaera R. Numerical modelling of partially filled aircraft fuel tanks submitted to Hydrodynamic Ram. Aerospace Science and Technology 16 (2011) 19–28.

[7] Varas D, Zaera R, López-Puente J. Experimental study of CFRP fluid-filled tubes subjected to high-velocity impact. Composite Structures 93 (2011) 2598–2609.

[8] Varas D, López-Puente J, Zaera R. Numerical Analysis of the Hydrodynamic Ram Phenomenon in Aircraft Fuel Tanks. AIAA Journal 50 (2012) 1621-1630.

[9] Artero-Guerrero JA, Pernas-Sánchez J, Varas D, López-Puente J. Numerical analysis of CFRP fluid-filled tubes subjected to high-velocity impact. Composite

Structures 96 (2013) 286–297.

[10] Cantwell WJ, Morton J. Detection of impact damage in CFRP laminates. Composites Structures 3 (1985) 241–257.

[11] Cantwell WJ, Morton J. Comparison of low and high velocity impact response of CFRP. Composites 20(6) (1989) 545–551.

[12] Cantwell WJ, Morton J. Impact perforation of carbon-fiber reinforced plastic. Composites Science and Technology 38(2) (1990) 119–141.

[13] Lee SWR, Sun CT. Dynamic penetration of graphite/epoxy laminates impacted by a blunt-ended projectile. Composites Science and Technology 49(4) (1993) 369–380.

[14] Sun CT, Potti SV. A simple model to prredict residual velocity of thick composite laminates subjected to high velocity impact. International Journal of Impact Engineering 18(3) (1996) 339–353.

[15] Larsson F, Damage tolerance of a stitched carbon/epoxy laminate. Composites Part A: applied science and manufacturing 28 (1997) 923–934.

[16] Hou JP, Petrinic N, Ruiz C, Hallett SR. Prediction of impact damage in composite plates. Composites Science and Technology 60:2, (2000) 273-281.

[17] López-Puente J, Zaera R, Navarro C. High energy impact on woven laminates.

[18] Fernández-Fdz D, López-Puente J, Zaera R. Prediction of the behaviour of CFRPs against high-velocity impact of solids employing an artificial neural network methodology. Composites Part A: applied science and manufacturing 39 (2008) 989–996.

[19] Turon A, Camanho PP, Costa J, Dávila CJ. A damage model for the simulation of delamination in advanced composites under variablemode loading. Mechanics

of Materials 38:11 (2006) 1072-1089.

[20] López-Puente J, Li S. Analysis of strain rate sensitivity of carbon/epoxy woven composites. International Journal of Impact Engineering 48 (2012) 54–64.

[21] Varas D, Artero-Guerrero JA,Pernas-Sánchez J, López-Puente J. Analysis of high velocity impacts of steel cylinders on thin carbon/epoxy woven laminates. Composite Structures 95 (2013) 623–629.

[22] Sun CT, Potti V. A simple model to predict residual velocities of thick composite laminates subjected to high velocity impact. International Journal of Impact Engineering 18(3) (1996) 339–353.

[23] Caprino G, Lopresto V, Santoro D. Ballistic impact behaviour of stitched graphite/epoxy laminates. Composites Science and Technology 67 (2007) 325–335.

[24] López-Puente J, Zaera R, Navarro C. An analytical model for high velocity impacts on thin cfrps woven laminates. International Journal of Solids and Structures 44 (2007) 2837-2851.

[25] López-Puente J, Varas D, Loya JA, Zaera R. Analytical modelling of high velocity impacts of cylindrical projectiles on carbon/epoxy laminates. Composites Part A: applied science and manufacturing 40 (2009) 1223–1230.

[26] Garcia-Castillo, SK, Sanchez-Saez, S, López-Puente J, Barbero, E, Navarro, C. Impact behaviour of preloaded glass/polyester woven plates. Composites Science and Technology 69(6) (2009) 711–717.

[27] Bland PW, Dear JP. Observations on the impact behaviour of carbon-fibre reinforced polymers for the qualitative validation of models. Composites Part A: applied science and manufacturing 32 (2001) 1217–1227.

[28] López-Puente J, Zaera R, Navarro C. The effect of low temperatures on the intermediate and high velocity impact response of CFRP. Composites: Part B

33 (2002) 559–566.

[29] Will MA, Franz T, Nurick GN. The effect of laminate stacking sequence of CFRP filament wound tubes subjected to projectile impact. Composites Structures 58 (2002) 259–270.

[30] Tanabe Y, Aoki M, Fujii K, Kasano H, Yasuda E. Fracture behavior of cfrps impacted by relatively high-velocity steel sphere. International Journal of Impact Engineering 28 (2003) 627–642.

[31] Zhao G, Cho C, Lu S, Wang Z. Experimental Study on Impact Resistance Properties of T300/Epoxy Composite Laminates. Journal of Composite Materials 44(7) (2010) 857–870.

[32] López-Puente J, Zaera R, Navarro C. Experimental and numerical analysis of normal and oblique ballistic impacts on thin carbon/epoxy woven laminates. Composites Part A: applied science and manufacturing 39 (2008) 374–387.

[33] Hazell PJ, Kister G, Stennett C, Bourque P, Cooper G. Normal and oblique penetration of woven CFRP laminates by a high velocity steel sphere. Composites Part A: applied science and manufacturing 39 (2008) 866–874.

[34] Hazell PJ, Appleby-Thomas GJ, Kister G. Impact, penetration, and perforation of a bonded carbon-fibre-reinforced plastic composite panel by a high-velocity steel sphere: an experimental study. The Journal of Strain Analysis for Engineering Design 45(6) (2010) 439–450.

[35] Ulven C, Vaidya UK, Hosur MV. Effect of projectile shape during ballistic perforation of VARTM carbon/epoxy composite panels. Composite Structures 61 (2003) 143–150.

[36] Reyes Villanueva G, Cantwell WJ. The high velocity impact response of composite and FML-reinforced sandwich structures. Composites Science and Technology 64 (2004) 35–54.

[37] Wang B, Xiong J, Wang X, Ma L, Zhang GQ, Wu LZ, Feng JC. Energy absorption eficiency of carbon fiber reinforced polymer laminates under high velocity impact. Materials and Design 50 (2013) 140–148.

[38] Sebaey TA, González EV, Lopes CS, Blanco N, Costa J. Damage resistance and damage tolerance of dispersed CFRP laminates: effect of ply clustering. Composite Structures 106 (2013) 96–103.

[39] Maimí P, Camanho PP, Mayugo JA, Dv́ila CG. A continuum damage model for composite laminates: Part II - Computational implementation and validation. Mechanics of Materials 39 (2007) 909–919.